PRAMANA — journal of physics

Vol. 85, No. 2
August 2015
pp. 303–313

Fission fragment mass and angular distributions: Probes to study non-equilibrium fission

R G THOMAS
Nuclear Physics Division, Bhabha Atomic Research Centre, Trombay, Mumbai 400 085, India
E-mail: rgthomas@barc.gov.in

DOI: 10.1007/s12043-015-1044-2; ***e*Publication:** 22 July 2015

Abstract. Synthesis of heavy and superheavy elements is severely hindered by fission and fission-like processes. The probability of these fission-like, non-equilibrium processes strongly depends on the entrance channel parameters. This article attempts to summarize the recent experimental findings and classify the signatures of these non-equilibrium processes based on macroscopic variables. The importance of the sticking time of the dinuclear complex with respect to the equilibration times of various degrees of freedom is emphasized.

Keywords. Fission; non-equilibrium fission; equilibration time.

PACS No. 25.70.Jj

1. Introduction

Synthesis of heavier and heavier elements using heavy-ion-induced reactions is severely hindered by fission and fission-like processes [1,2]. A major hurdle in superheavy element production is the presence of non-equilibrium processes such as fast fission (FF) [3,4], quasifission (QF) [5–11] and pre-equilibrium fission (PEF) [12,13]. As these processes (often commonly called quasifission in the literature) differ subtly in terms of the observables which are measured in a reaction, and disentangling the contributions of each of these processes is very challenging. While FF is observed when the fission barrier becomes vanishingly small at very high angular momenta, quasifission occurs when the trajectories bypass the saddle point (fission barrier) when the charge product of the colliding nuclei exceeds a certain value. PEF, on the other hand corresponds to reseparation after passing the saddle point but before forming a compact compound nucleus (CN) when the temperature of the system becomes comparable to the fission barrier. Though, it is known that the probability of these non-equilibrium processes depends on the entrance channel properties of the colliding nuclei, a quantitative description is still unavailable. Dynamical models proposed in the 1980s by Swiatecki and others, have predicted the onset of quasifission when charge product (Z_1Z_2) exceeds 1600. However, recent

measurements have shown that evidence of non-equilibrium fission can be found in systems with charge product as low as 540 [13,14].

In the following, we shall attempt to classify various non-equilibrium fission-like processes based on certain parameters related to the entrance channel. The manifestation of these non-equilibrium processes is found to vary dramatically with respect to the target–projectile combination, mass asymmetry of the entrance channel, static deformation of the colliding partners, and the bombarding energy. The signatures of non-equilibrium fission are: (i) strong mass–angle correlation in the mass–angle distribution of fission fragments, (ii) broader mass distributions compared to that of CN fission and (iii) anomalously large angular anisotropies compared to the statistical model predictions. It should be noted that the presence of any of these characteristics will qualify the process to be non-equilibrium. In the following discussion, we shall attempt to broadly classify the nuclear landscape (what we call C–T fissility plot [14]) based on the manifestations of these signatures.

2. The C–T fissility plot

According to the macroscopic model of Swiatecki and others [6–8], the dynamic evolution of the dinuclear system after contact is principally governed by the multidimensional potential energy surface (PES) of the combined system described by the three variables, viz., the radial separation, the neck radius and the mass asymmetry of the fragments. While the choice of the variables may vary with the models [15], the dynamics are depicted by three milestone configurations viz., the contact configuration, the conditional saddle point and the unconditional saddle point. The location of these points on the PES, and the injection point onto this multidimensional surface plays a crucial role in the subsequent evolution of the composite system. From the experimental observations in the 1980s, Blocki *et al* [8] have parametrized the onset of quasifission using a macroscopic variable called mean fissility given by $\chi_{\rm m} = \frac{1}{3}\chi_{\rm eff} + \frac{2}{3}\chi_{\rm CN}$, which incorporates the target–projectile and CN fissilities:

$$\chi_{\rm eff} = (Z^2/A)_{\rm eff}/(Z^2/A)_{\rm crit} \tag{1}$$

with

$$(Z^2/A)_{\rm eff} = 4Z_1Z_2/(A_1^{1/3}A_2^{1/3}(A_1^{1/3} + A_2^{1/3})) \tag{2}$$

while the CN fissility is

$$\chi_{\rm CN} = (Z^2/A)/(Z^2/A)_{\rm crit}, \tag{3}$$

where

$$(Z^2/A)_{\rm crit} = 50.883(1 - 1.7826I^2), \tag{4}$$

with $I = (A - 2Z)/A$.

From the analysis of Blocki *et al*, it was found that $\chi_{\rm m} = 0.72$ marks the onset of the need for extra push energy (excess energy over the Coulomb barrier) to achieve fusion. It was also noticed that the manifestation of the non-equilibrium nature of the re-separation process on the mass and spatial distributions of the fragments depends critically on the sticking time $\tau_{\rm s}$ of the dinuclear system compared to the characteristic equilibration time $\tau_{\rm M}$ ($\sim 5 \times 10^{-21}$ s) of mass degree of freedom.

2.1 *The C–T fissility plot*

Figure 1 shows the plot of entrance channel fissility (χ_{eff}) vs. the CN fissility (χ_{CN}) (referred to as C–T fissility plot). Different targets are characterized by arcs whereas projectiles are described by lines cutting the arcs for various target–projectile combinations. $Z_1 Z_2 \geq 1600$ (thick red line) and $\chi_{\text{m}} = 0.72$ (solid blue line) are also shown in the plot. The onset of non-equilibrium fission can be very well classified into different regions in this plot. The locus of $\alpha = \alpha_{\text{BG}}$ for different composite systems are shown by the thick black curve. α_{BG} is calculated by the following equation [16]:

$$\alpha_{\text{BG}} = p\sqrt{\frac{x - x_{\text{BG}}}{(x - x_{\text{BG}}) + q}}, \tag{5}$$

where $x_{\text{BG}} = 0.396$, $p = 1.12$ and $q = 0.24$. For this calculation, following Blocki *et al* [8], we have considered the charge-to-mass ratio of the target and the projectile to lie along the valley of beta stability as approximated by the Green's formula,

$$Z/A = \frac{1}{2}[1 - 0.4A/(200 + A)]. \tag{6}$$

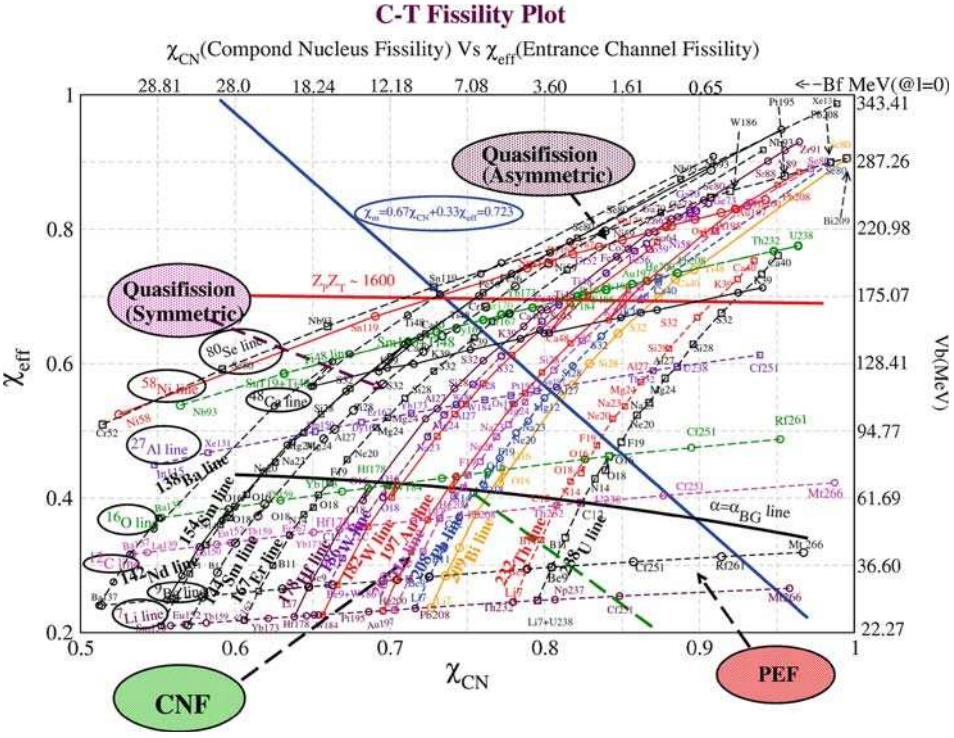

Figure 1. Plot of entrance-channel fissility (χ_{eff}) vs. CN fissility (χ_{CN}) for various target–projectile combinations. The onset of non-equilibrium fission is shown in different fissility regions.

For a given pair of nuclei with mass numbers A_1 and A_2, we first calculate the corresponding atomic numbers according to eq. (6) and the sum of these numbers is the total atomic number Z, which is then divided between the two fragments in the ratio of their masses, viz., $Z_i = A_i(Z/A)$. We also show on the right-hand side of figure 1, the Coulomb barrier obtained using the parametrization following Swiatecki [17], given by

$$V_b = 0.85247 \times z + 0.001361 \times z^2 - 0.00000223 \times z^3 \text{ MeV}, \tag{7}$$

where $z = Z_1Z_2/(A_1^{1/3} + A_2^{1/3})$. On the top, along the x-axis, the liquid-drop fission barrier is also shown for the corresponding fissility [18]. The thick solid curves or lines on the C–T fissility plot are individually discussed below:

(a) Z_1Z_2 line. The red solid line shows the line where the entrance channel charge product exceeds the limit of 1600, a theoretical prediction of early 1980s. Experimentally, in early 1980s this prediction was well established [9–11] where strong mass–angle correlation was observed. However, many recent experiments have reported strong mass–angle correlation in reactions where $Z_1Z_2 \sim 1300$ [19].

(b) $\chi_m = 0.72$ line. The blue solid line is the mean fissility line, the system beyond this line exceeds this limit. As discussed earlier, this limit of mean fissility marks the onset of quasifission according to the model by Blocki [8]. It is found that systems exceeding this limit exhibit strong mass–angle correlation indicating the strong presence of fission before mass equilibration.

(c) $\alpha = \alpha_{BG}$ line. The thick black curve gives $\alpha = \alpha_{BG}$ line. All the systems with entrance channel mass asymmetry (α) more than or equal to Bussinaro–Gallone (BG) critical mass asymmetry (α_{BG}, a point where potential is maximum for a given fissility) rapidly evolves to a mononuclear system to form compact CN (marked CNF in the fissility plot). On the other hand, systems with $\alpha < \alpha_{BG}$ evolves towards dinuclear shapes. The green dashed line indicates the shifted $\alpha = \alpha_{BG}$ line when one of the collision partners is statically deformed.

3. Characteristics of equilibrium fission

Equilibrium fission is characterized by the formation of a CN which is equilibrated in all degrees of freedom. The mass, energy and angular distribution of fragments are expected to exhibit properties which are independent of the entrance channel [20].

3.1 *Mass–TKE distributions*

There have been extensive measurements on the mass and kinetic energy distribution of fission fragments in heavy-ion-induced reactions. Based on these observations, the mass distribution from the fission of a CN formed at moderate excitation energies ($E^* = 30-80$ MeV) is well described by a Gaussian peaking around symmetric mass division, and with a variance depending linearly on the temperature and the square of the angular momentum [21–25]:

$$\sigma_A^2 = \mu T + \nu\langle l^2\rangle, \tag{8}$$

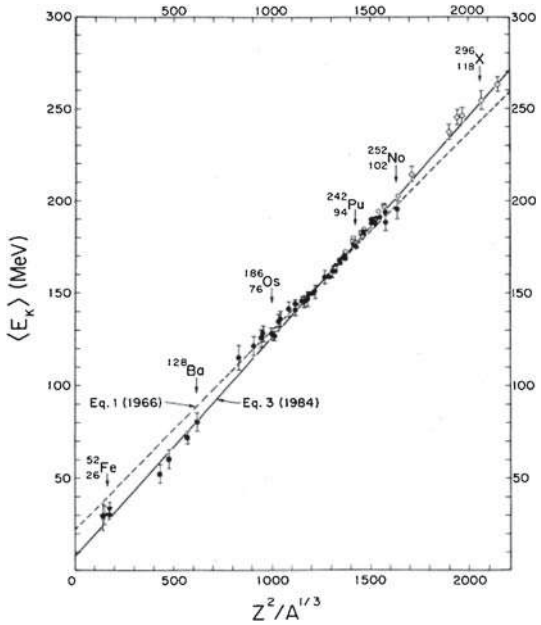

Figure 2. The average kinetic energy shows a remarkable dependence on the charge and mass of the composite system and is independent of the entrance-channel parameters (figure taken from [26]).

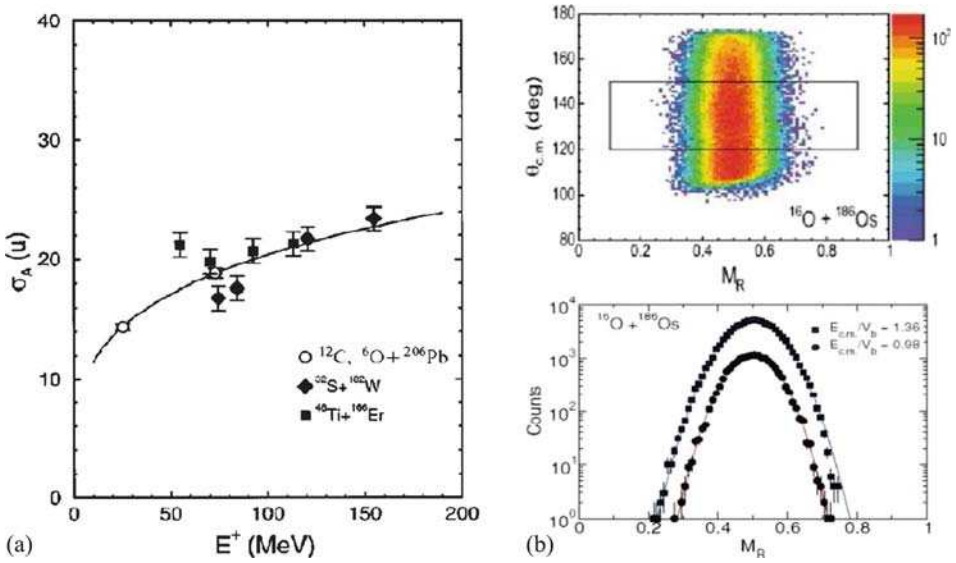

Figure 3. (**a**) The dependence of the variance of mass distribution on the temperature of the fissioning system (figure taken from [21]). (**b**) The mass–angle distribution showing no dependence of angle of emission and mass split in CN fission (figure taken from [19]).

where T is the transition state temperature, l is the angular momentum and μ and ν are constants for a given compound system. The average kinetic energy of the fragments is found to depend on the charge and mass of the CN and independent of the entrance-channel properties. The Viola systematic gives remarkably close estimate of the experimentally obtained $\langle TKE\rangle$ over the entire range of fissility [26]. The $\langle TKE\rangle$ of a number of systems along with the Viola systematic [26] is plotted in figure 2. Figure 3a shows the variance of mass distribution as a function of excitation energy for different systems, along with the fit using eq. (8). The mass distribution and the mass–angle correlation for ^{16}O $+^{186}$Os are shown in figure 3b, which depicts the general features observed for the compound nucleus fission reactions.

3.2 *Statistical saddle-point model for angular distribution*

Statistical saddle-point model (SSPM) or transition-state model (TSM) explains the angular distribution of fission fragments from the system undergoing the CN fission [20]. The angular distribution may be given as

$$W(\theta) = \sum (2J+1)T_J \sum \rho_J(K)|d^J_{MK}(\theta)|^2, \tag{9}$$

where J is the spin of the nucleus, K is its projection onto the symmetry axis, T_J is the transmission coefficient for fusion with spin I, $\rho_J(K)$ is the probability of spin projection K for total spin J and $d^J_{MK}(\theta)$ is the rotor wave function.

To a good approximation the angular anisotropy A, defined as the ratio of yield at 180° or 0° to that at 90° with respect to beam axis, is given by the following expression:

$$A = 1 + \langle l^2\rangle/4K_0^2, \tag{10}$$

where K_0^2 is the variance of Gaussian K-distribution peaked at $K = 0$. It can also be shown that K_0^2 is proportional to the effective moment of inertia at the saddle point and the temperature at the saddle point [20]. Figure 4 shows the angular distributions in ^{16}O+^{208}Pb reaction which is well described by the standard statistical model.

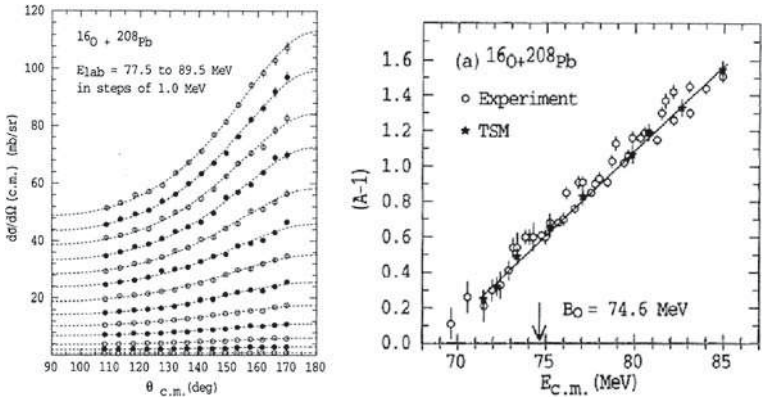

Figure 4. Fission fragment angular distributions described by the statistical model in CN fission (figure taken from [27]).

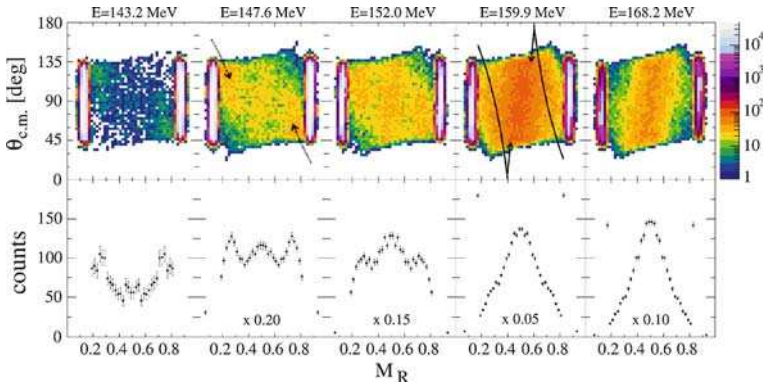

Figure 5. Strong mass–angle correlation observed in ^{32}S+^{232}Th reaction. The appearance of asymmetric component in projected mass ratio distribution at sub-barrier energies can be seen (figure taken from [28]).

4. Characteristics of non-equilibrium fission

4.1 *Strong mass–angle correlations*

A distinct characteristic of the presence of quasifission is the strong mass–angle correlation in mass–angle distribution (MAD) of fission fragments. The strong mass–angle correlation arises due to the incomplete drift in the mass degree when the system reseparates even before the completion of one rotation. Such strong mass–angle correlations are observed for heavy target–projectile combinations shown beyond the red thick line in the C–T fissility plot. Recent MAD measurement on ^{32}S+^{232}Th system at below- and above-barrier energies [28], show two distinct features in mass splits at sub-barrier and above-barrier energies (figure 5). Mass–angle distribution measurements in less fissile systems, for example ^{48}Ti +^{154}Sm [19] and ^{48}Ti+^{170}Er [29] systems (figure 6), also show notable mass–angle correlation where the charge product Z_1Z_2 was much less than 1600. Therefore, one may say that systems that lie above the $\chi_m = 0.72$ line show evidence of non-equilibrium fission in terms of strong mass–angle correlations (quasifission-asymmetric in the C–T fissility plot).

4.2 *Broader mass distributions*

For composite systems with longer sticking times, greater than that required to undergo one full rotation, the correlation of mass splits with respect to emission angle vanishes. Mass–angle distribution in this case will be symmetric around the mass ratio ($M_R = 0.5$) and it is very similar to fusion–fission mass distribution. However, there may be enhancement in the width of mass distribution as compared to the width expected for fusion–fission reaction.

Many recent experiments [19,29–31] have shown the increase in width of fission fragment mass distribution as compared to the width expected for fusion–fission. These measurements (the reactions indicated in figure 7) do not indicate any mass–angle correlation in mass–angle distribution (a typical example of MAD in this case [30] is shown in figure 8), but the widths of mass distributions are found to be broader for more

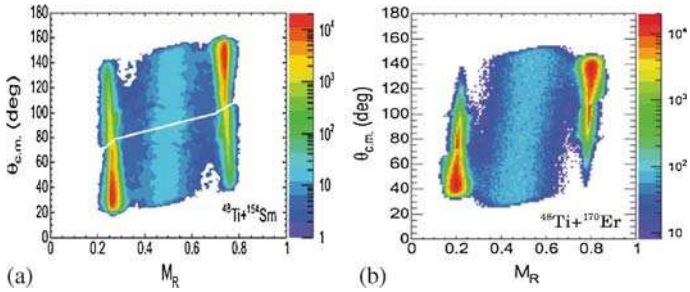

Figure 6. Mass–angle correlation observed in ^{48}Ti-induced reactions on (**a**) ^{154}Sm and (**b**) ^{170}Er targets.

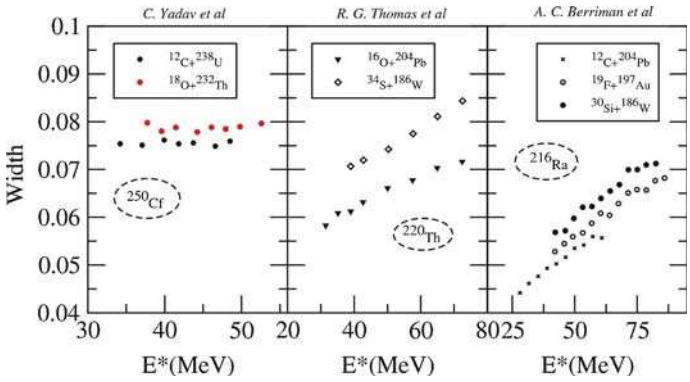

Figure 7. Width as a function of CN excitation energies for various systems obtained from [29–31].

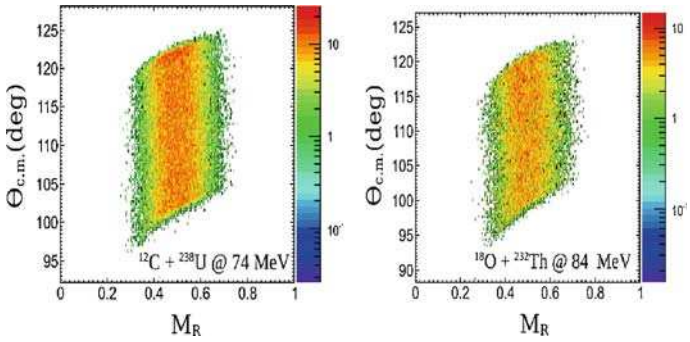

Figure 8. Plot showing mass–angle distribution of full momentum transfer events for two systems forming the ^{250}Cf CN at the indicated laboratory energies. Both do not show any mass–angle correlation at all energies studied [30].

symmetric reactions forming the same CN. The experimental widths obtained from [29–31] plotted as a function of excitation energies of CN are shown in figure 7. These apparent broadening of mass distributions were attributed to the presence of a small fraction of non-equilibrated mass asymmetry degree of freedom, the characteristic time for

mass equilibration, τ_M being $\sim 5 \times 10^{-21}$ s. Systems belonging to this class of non-equilibrium fission (quasifission-symmetric) is indicated in the C–T fissility plot towards the top-left side.

4.3 *Anomalous angular distributions*

The standard statistical model successfully explains the angular distribution of a large number of systems at moderate excitation energies [20]. However, a large number of systems, particularly the ones involving actinide targets exhibit anomalously large anisotropies in the angular distribution of fission fragments. It is also interesting to note that these systems do not show any strong evidence of mass non-equilibration. However, from the anomalously large anisotropies, one may conclude that these systems re-separate before the characteristic K-equilibration time (τ_K) $\sim 10^{-20}$ s. This led to an alternate explanation given by Ramamurthy and Kapoor [12] where it was proposed that anomalous fission fragment anisotropy can arise due to an admixture of compound nucleus events and non-compound fission events, where K-degree of freedom is not fully equilibrated. This mechanism, called the pre-equilibrium fission (PEF) is expected to be dominant in situations where temperature is comparable or higher than the fission barrier height. These kinds of events are visible for those systems for which the entrance channel mass asymmetry, α, is less than the critical value α_{BG}. Direct experimental evidence of entrance channel-dependent fission fragment anisotropy was observed in ^{11}B, ^{12}C, ^{16}O, ^{19}F $+^{232}$Th and ^{237}Np systems at near and sub-barrier energies [32–34].

In [13], it is shown that PEF can occur even for the reactions with $\alpha > \alpha_{BG}$ at near and sub-barrier energies as the Bussinaro–Gallone critical mass asymmetry (α_{BG}) shifts towards the higher mass asymmetry due to elongated touching configuration at sub-barrier energies. This shift in α_{BG} due to large static deformation of actinide targets is shown by thick dashed green line in figure 1. Figure 9 shows the anistropy plots for $\alpha > \alpha_{BG}$ systems where the PEF model [13] successfully explains the experimental results.

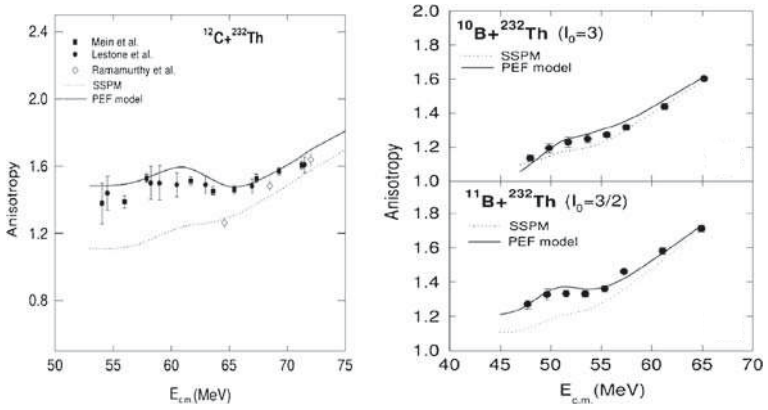

Figure 9. Calculated fission fragment anisotropy on the basis of SSPM and PEF models along with the experimental results for systems with $\alpha > \alpha_{BG}$ are shown (figure adopted from [13]).

5. Summary

Fission-like non-equilibrium mechanisms are extensively studied worldwide after their first experimental observation in the early 1980s, where it was recognized that the fission fragments produced in heavy-ion-induced reactions may not always originate from equilibrium fission decay of compound nucleus. Since then, different observables like mass–angle correlation, fission fragment angular anisotropy and fission fragment mass width were used as probes to investigate the presence of non-equilibrium fission processes. The experimental observables in non-equilibrium fission are found to crucially depend on the interaction time (sticking time) of the dinuclear complex with respect to the characteristic relaxation time of various degrees of freedom, before it decays into binary fission-like fragments. This interaction time in turn depends on the entrance-channel parameters of the colliding nuclei. Thus, a system that remains together for a time comparable to or shorter than τ_M (quasifission-asymmetric) exhibits strong mass–angle correlations, large mass widths and large anisotropies. Systems whose sticking time is between τ_M and τ_K may not show any significant correlation of mass with angle but can show broadened mass distributions and large angular anisotropies (quasifission-symmetric). However, systems that stick together for time-scales comparable to τ_K but reseparate before reaching a CN may not exhibit any signs of incomplete relaxation of mass but can still exhibit angular anisotropies larger than predicted by the TSM for the CN fission (pre-equilibrium fission). A comprehensive theoretical formalism is very much in need to quantitatively understand the experimental observations.

Acknowledgements

The author would like to thank S S Kapoor for many illuminating discussions and valuable suggestions. He also thanks R K Choudhury and A K Mohanty for many fruitful discussions. The help received from Chandrabhan Yadav in the preparation of this article is gratefully acknowledged.

References

[1] Yuri Ts Oganessian and Yuri A Lazarev, *Treatise on heavy-ion science* edited by D A Bromley (Plenum, New York, 1985) Vol. 4, p. 3
[2] Peter Armbruster, *C. R. Phys.* **4**, 571594 (2003)
[3] C Lebrun, F Hanappe, J F Lecolley, F Lefebvres, C Ngo, J Peter and B Tamain, *Nucl. Phys. A* **321**, 207 (1979)
[4] J Peter and B Tamain, *Nucl. Phys. A* **321**, 207 (1979)
B Borderie *et al*, *Z. Phys. A* **299**, 263 (1981)
[5] Peter Moller and Arnold J Sierk, *Nature* **422**, 485 (2003)
[6] W J Swiatecki, *Phys. Scr.* **24**, 113 (1981)
[7] S Bjornholm and W J Swiatecki, *Nucl. Phys. A* **391**, 471 (1982)
[8] J P Blocki *et al*, *Nucl. Phys. A* **459**, 145 (1986)
[9] J Toke *et al*, *Nucl. Phys. A* **440**, 327 (1985)
[10] R Bock *et al*, *Nucl. Phys. A* **388**, 334 (1982)
[11] W Q Shen *et al*, *Phys. Rev. C* **36**, 115 (1987)

[12] V S Ramamurthy and S S Kapoor, *Phys. Rev. Lett.* **54**, 178 (1985)
[13] R G Thomas, R K Choudhury, A K Mohanty, A Saxena and S S Kapoor, *Phys. Rev. C* **67**, 041601(R) (2003)
[14] R K Choudhury and R G Thomas, *J. Phys.: Conf. Ser.* **282**, 012004 (2011)
[15] P Moller *et al*, *Nature* **409**, 785 (2001)
[16] M Abe, KEK Report No. 86-26, KEK TH-28 (1986)
[17] W J Swiatecki *et al*, *Phys. Rev. C* **71**, 014602 (2005)
[18] A J Sierk, *Phys. Rev. C* **33**, 2039 (1986)
[19] R Rafiei, R G Thomas, D J Hinde, M Dasgupta, C R Morton, L R Gasques, M L Brown and M D Rodriguez, *Phys. Rev. C* **77**, 024606 (2008)
[20] R Vandenbosch and J R Huizenga, *Nuclear fission* (Acadamic, New York, 1973)
[21] B B Back *et al*, *Phys. Rev. C* **53**, 1734 (1996)
[22] R K Choudhury *et al*, *Phys. Rev. C* **60**, 054609 (1999)
[23] M G Itkis and A Ya Rusanov, *Phys. Part. Nuclei* **29**, 160 (1998)
[24] G D Adeev, I I Gontchar, V V Pashkevich, N I Pischasov and O I Serdyuk, *Phys. Part. Nuclei* **19**, 1229 (1988)
[25] G N Knyazheva *et al*, *Phys. Rev. C* **75**, 064602 (2007)
[26] V E Viola, K Kwiatkowski and M Walker, *Phys. Rev. C* **31**, 1550 (1985)
[27] C R Morton *et al*, *Phys. Rev. C* **52**, 243 (1995)
[28] D J Hinde, R G Thomas, R du Rietz, A Diaz-Torres, M Dasgupta, M L Brown, M Evers, L R Gasques, R Rafiei and M D Rodriguez, *Phys. Rev. Lett.* **100**, 202701 (2008)
[29] R G Thomas, D J Hinde, D Duniec, F Zenke, M Dasgupta, M L Brown, M Evers, L R Gasques, M D Rodriguez and A Diaz-Torres, *Phys. Rev. C* **77**, 034610 (2008)
[30] C Yadav *et al*, *Phys. Rev. C* **86**, 034606 (2012)
[31] A C Berriman, D J Hinde, M Dasgupta, C R Morton, R D Butt and J O Newton, *Nature (London)* **413**, 144 (2001)
[32] V S Ramamurthy *et al*, *Phys. Rev. Lett.* **65**, 25 (1990)
[33] J C Mein, D J Hinde, M Dasgupta, J R Leigh, J O Newton and H Timmers, *Phys. Rev. C* **55**, R995 (1997)
[34] J P Lestone *et al*, *J. Phys. G* **23**, 1349 (1997)